SAND2023-12742J

Self-Adhesive Ionomers for Alkaline Electrolysis: Optimized Hydrogen Evolution Electrode

Hui Min Tee[1], Habin Park[1], Parin N. Shah[1], Jamie Trindell[2], Joshua Sugar [2], and Paul A. Kohl[1]

[1] Georgia Institute of Technology, Chemical and Biomolecular Engineering, Atlanta, GA 30332-0100 USA

2 Sandia National Laboratory, 7011 East Ave., Building 940 Room 1184, Livermore, CA 94550

Keywords: anion conductive ionomer, anion exchange membrane, electrode fabrication, vinyl addition, poly(norbornene), cross-linking, water electrolysis, hydrogen

*Contact author: kohl@gatech.edu, 404-894-2893

Abstract

Hydrogen produced through low-temperature water electrolysis using anion exchange membranes (AEM) combines the benefits of liquid-electrolyte alkaline electrolysis and solid-polymer proton exchange membrane electrolysis. The anion conductive ionomers in the oxygen-producing anode and hydrogen-producing cathode are a critical part of the three-dimensional electrodes. The ionomer in the hydrogen-producing cathode facilitates hydroxide and water conduction to the cathode catalyst particles from the hydroxide conducting membrane and binds the catalyst particles to the porous transport layer. In this study, the cathode durability was improved by use of a self-adhesive cathode ionomer to chemically bond the cathode catalyst particles to the porous transport layer. It was found that the cathode ionomers with high ion exchange capacity (IEC) were more effective than low IEC ionomers because of the need to transport water to the cathode catalyst and transport hydroxide away from the cathode. The cathode durability was improved by using ionomers which were soluble in the spray-coated cathode ink. Optimization of the catalyst and ionomer content within the cathode led to electrolysis cells which were both mechanically durable and operated at low voltage.

Introduction

Renewable energy can be used to supply significant global energy and provide energy independence. [1] However, renewable energy is inherently intermittent and requires an economical way of storing and converting the energy to a chemical form. Hydrogen produced via water electrolysis is a means of on-site chemical energy storage for renewable sources. Green hydrogen can be transported and used in chemical synthesis, heat engines or fuel cells.

Anion exchange membrane electrolyzers (AEMEL) are an attractive alternative to liquid-electrolyte alkaline electrolyzers (AEL) or solid-polymer proton exchange membrane electrolyzers (PEMEL). [2] The alkaline solid polymer electrolyte combines the advantages of an AEL and PEMEL. The alkaline environment provides a more facile oxygen evolution reaction (OER) using a non-platinum group metal (PGM) electrocatalysts. [2-12] It has been found that specific hydrocarbon-based solid polymers are stable at high pH, compared to low pH PEMEL membranes which require perfluorinated polymers. [13, 14] In addition, the solid polymer membrane lowers the overall electrolyzer cost by eliminating the need for electrolyte recirculation and allows for pressurized hydrogen to be produced during electrolysis. [1, 15-21]

In an AEMEL, hydroxide ions are oxidized at the oxygen-producing anode (i.e., positive electrode) and water is reduced at the hydrogen-producing cathode, as shown in Figure 1. Liquid water can be fed to the anode leaving the cathode to be run dry so that pressurized hydrogen gas can be produced without having to separate it from liquid water. [20, 22] During AEMEL operation, the liquid water fed to the anode diffuses from the anode to the cathode through the membrane. The activity of water at the cathode catalyst is controlled by the rate of water diffusion through the membrane and hydrophilicity of the cathode ionomer. Previous cathode ionomer studies successfully used solvent-insoluble, anion-conducting ionomers interspersed with the catalyst

particles on the porous transport layer (PTL). [23] Careful control of the cathode ionomer ion exchange capacity (IEC) led to low voltage electrolysis. It was shown that inadequate cathode water activity resulted in electrode dry-out which limited the rate of hydrogen production and degraded the electrode materials. [23]

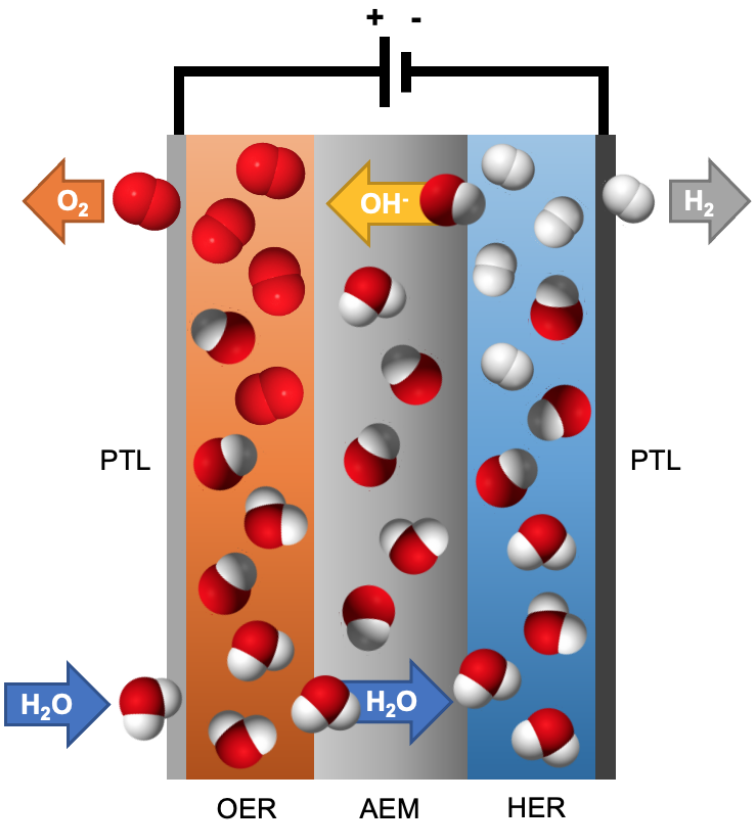

$$Anode: 4OH^- \rightarrow O_2 + 2H_2O + 4e^- \quad E_0 = 0.401\,V$$

$$Cathode: 4H_2O + 4e^- \rightarrow 2H_2 + 4OH^- \quad E_0 = -0.828\,V$$

$$Overall: 2H_2O \rightarrow 2H_2 + O_2 \quad E_0 = 1.23\,V$$

Figure 1. Low-temperature AEM electrolysis configuration.

The transport properties of anion exchange membranes (AEM) are competitive with proton exchange membranes (PEM) with conductivity >200 mS/cm, and excellent stability, durability and mechanical properties. [13-15] The cost-basis for AEMs is considerably lower than PEMs because hydrocarbon backbones can be used for AEMs compared to the perfluorinated polymers

used in PEMs. The ionomers used in alkaline electrolyzers has received less attention. [3, 17, 23, 24] It has been recognized that the hydrophobicity of the anode and cathode ionomer is critical to achieving high performance electrolysis. [3, 24, 25] The ionomers contained in the electrolyzer anode and cathode provide an ionic pathway between the AEM and the three-dimensional assembly of catalyst particles. This is more critical at the hydrogen-cathode than the oxygen-anode because a dilute aqueous electrolyte is usually fed to the oxygen-anode which also provides ionic conductivity. The hydrogen-cathode is usually operated dry without a supporting electrolyte which makes the ionomer the only ionic pathway between the membrane and catalyst. Although high ionic conductivity is desirable, it is recognized that high water uptake (WU) can swell the ionomer and disrupt the transport of water, hydroxide and hydrogen gas. In addition to ionic and water transport, the ionomer binds the catalyst to the porous transport layer (PTL) and membrane. This is especially important for gas evolving electrolyzers due to the forces created during the volumetric expansion of the liquid water to a gas. [3, 24, 25] Previous studies formed the AEM electrodes by spraying catalyst and ionomer particles suspended in a solvent (i.e., electrode ink) onto the PTL. The ionomers were insoluble in the ink solvent because they were already in the ion-conducting form and sometimes cross-linked. [3, 24] Both attributes contribute to their insolubility. The resulting electrodes were a mixture of closely packed ionomer and catalyst particles. This method of electrode fabrication is referred to as the ‘particle-cast’ method in this report. The catalyst particles were held in place by physical adhesion, such as hydrogen bonding.

In this study, a different approach was investigated for forming the hydrogen-evolving cathode in the AEMEL. Rather than creating a suspension of insoluble catalyst and ionomer particles in the electrode ink, a soluble form of the ionomer was incorporated into the electrode ink. This method is referred to as the ‘solvent-cast’ method. This was achieved by dissolving the

cathode ionomer in the ink before the ionomer polymer was converted into an anion conducting salt. Further, a family of poly(norbornene) terpolymers with a range of IEC values were synthesized for use as ionomers. The terpolymers were composed of a hydrophobic norbornene monomer, an alkyl bromine norbornene monomer, and a carboxylic acid norbornene monomer. In addition, a bis-phenol-A-diglycidyl ether adhesive was added to the cathode ink to chemically bond it to the catalyst surface, PTL and carboxylic acid monomer within the ionomer. In this way, rather than simply mixing insoluble catalyst and ionomer particles in the hydrogen electrode, the ionomer and adhesive were evenly distributed within the electrode. Although significant improvement in adhesion could be envisioned by coating the catalyst and PTL with adhesive and ionomer, this could also lead to catalyst deactivation due to polymer coverage. In this study, the properties and performance of the self-adhesive ionomer in the hydrogen electrode were investigated and optimized.

Experimental

Polymer Synthesis: Poly(norbornene) terpolymers were synthesized and characterized by the method previously reported by Mandal et al. [13, 14] Briefly, the terpolymer was synthesized in a vinyl-addition polymerization reaction using butyl norbornene (BuNB), bromobutyl norbornene (BBNB) and norbornene propionic acid ethyl ester (NBPEE). After synthesis, the NBPEE was converted into a pendant carboxylic acid by reaction with concentrated HCl. The BBNB was later quaternized with trimethyl amine (TMA) or used to lightly cross-link the polymer by using N,N tetramethyl hexadiamine (TMHDA). In this report, the terpolymers are named by their mole ratio of BuNB (hydrophobic monomer):BBNB (ion conducting monomer):NBPEE (adhesive ionomer). For example, 20:60:20 ionomer has 20 mol% BuNB, 60 mol% BBNB and 20 mol% NBPEE. The IEC of the ionomer was determined by controlling the mole fraction of BuNB

in the terpolymer. IEC for each ionomer was calculated based on ^{1}H NMR analysis using a Bruker Avance 400 MHz NMR instrument using d-tetra hydro furan (d-THF) as the solvent. The number average molecular weight (M_n) and dispersity index (Đ) of the polymers were measured by gel permeation chromatography (GPC) on a Shimadzu GPC (DGU-20A, LC-20AD, CTO-20A, and RID-20A), a Shodex column (KF-804L), with HPLC grade THF (1 mL/min flow rate at 30 °C) eluent and calibrated against a polystyrene standard as previously described.

The anion exchange membranes used in this study were formed by casting the BuNB, BBNB copolymer into a film with a proprietary polymer reinforcement (Pention®, Xergy Inc.). 5 mol% TMHDA cross-linker was used relative to the mol% of the halogenated monomers in the polymer. In this report, the membranes are named GTXX-Y, where XX is the mole percent ion conducting BBNB in the polymer and Y is the mole percent cross-linker, with respect to the available bromo butyl sites in the polymer.

Electrode Preparation: The solvent-cast and particle-cast anodes and cathodes were fabricated by using an airbrush to spray catalyst ink directly onto the porous transport layer PTL. The baseline solvent-cast cathode electrode ink formulation used 50 mg of ionomer stirred in 8 ml THF until dissolved. 8 mg of a EPON 826 bis(phenol)-A-diglycidyl ether epoxy adhesive binder (epoxy equivalent weight 180 g/eq) dissolved in THF and 100 mg of Pt_3Ni on ECS-3701 (Pajarito Powder) was added to the THF ionomer solution and sonicated in an ice bath for 1 h. The slurry was sprayed onto carbon paper PTL resulting in catalyst, epoxy binder mixture, and ionomer loading of 1.2 mg/cm^2, 0.31 mg/cm^2, 0.1 mg/cm^2, respectively. The same solvent-cast fabrication method was used for the anode using a 50:30:20 (BuNB:BBNB:BDNB ratio) terpolymer and nickel ferrite catalyst ($NiFe_2O_4$, Pajarito Powder). The anode ink was sprayed onto a stainless steel PTL resulting in catalyst, epoxy binder mixture and ionomer loading of 0.7

mg/cm^2, 0.11 mg/cm^2 and 0.16 mg/cm^2, respectively. The respective solvent-cast anode and cathode PTL and electrode loading densities for the catalyst, epoxy binder mixture and ionomer were used throughout this study unless otherwise noted.

The baseline particle-cast cathode ink formulation used cross-linked GT72-3 (72 mol% BBNB, 28 mol% BuNB) poly(norbornene) copolymer with 3 mol% of the available head-groups cross-linked with TMHDA). 25 mg of dry ionomer was ground in a mortar and pestle for 5 min. 1.3 ml of deionized water was added and ground for 1 min. 100 mg of 30 wt% Pt_3Ni on ECS-3701 catalyst was added to the mortar and ground for another 5 min followed by the addition of 8 mg EPON 826 bis(phenol)-A-diglycidyl ether epoxy adhesive binder (epoxy equivalent weight 180 g/eq) dissolved in acetone. The mixture was ground for 5 min followed by the addition of 12 ml isopropanol to the slurry. The ink is transferred to a vial and sonicated for 1.5 h in an ice bath. The cathode ink was sprayed onto carbon paper PTL resulting in catalyst, epoxy binder mixture, and ionomer loading of 0.7 mg/cm^2, 0.06 mg/cm^2 and 0.18 mg/cm^2, respectively. These loading densities for the catalyst, epoxy binder mixture and ionomer were used through this study for the particle-cast cathode electrode fabrication unless otherwise noted.

Membrane Electrode Assembly (MEA) fabrication: The membrane electrode assemblies (MEAs) were made by cutting electrodes (4 cm^2) from the larger, 16 cm^2 anode and cathode sheets. The AEM (5 cm^2), cathode and anode were individually ion exchanged to the OH^- form by soaking in 1.5 M NaOH solution for a total of 60 min refreshing the base solution every 20 minutes prior to cell assembly. A nitrogen cover gas was applied during the entire ion exchange to avoid carbonation from atmospheric CO_2. The AEM was placed between the two electrodes and pressed together in the 5 cm^2 Fuel Cell Technologies hardware between two 316 stainless steel single-pass

serpentine flow-fields and 10 mil Tefzel gaskets. The torque applied to the cell hardware was 25 in-lb.

Electrolyzer Testing: Aqueous 0.1 M NaOH was recirculated to the anode at 60°C during operation. The cell was conditioned at 60°C for 30 min and held at 0.1 A/cm^2 for 30 min. The current density was gradually increased to 0.75 A/cm^2 or 1 A/cm^2, after which, an impedance spectrum at 1.3 V was recorded using a PARSTAT 2263 potentiostat over a frequency range of 10 mHz to 100 kHz. The polarization curve was recorded on a Metrohm Autolab B.V. type PGSTAT204 potentiostat with a linear sweep voltammetry (LSV) technique. The steady state polarization curve was recorded by holding the voltage at a series of constant current densities. The cell voltage was recorded as a function of time at constant current for the durability tests.

Results and Discussion:

The particle-cast electrodes for alkaline polymer electrolysis were made by spraying an ink, containing an insoluble ionomer and a catalyst, onto a PTL. [3, 24] The particle-cast ionomer was not soluble in the ink because it was in the quaternary ammonium halide form, having been previously aminated by a reaction of the pendant butyl bromide moiety with TMA, or other tertiary amine, such as the TMHDA cross-linker. The aminated ionomer was first ground to a fine powder and applied as a suspension to the PTL. This particle-cast electrode was compared to the solvent-cast cathode fabrication method which used a soluble ionomer in the ink. The ionomer was soluble in THF because it was in the butyl bromide form before amination with TMA. In addition, the solvent-cast ionomer was a terpolymer, containing a carboxylic acid moiety. In addition to the catalyst and ionomer in the inks, prepared with the both methods, bis-(phenol-A-diglycidyl ether) was added as an adhesive for chemically bonding the ionomer, catalyst, and PTL together. Figure 2 shows the steady-state voltage response at 0.75 A/cm^2 for

the particle-cast and solvent-cast cathodes using otherwise identical components including AEM and anode.

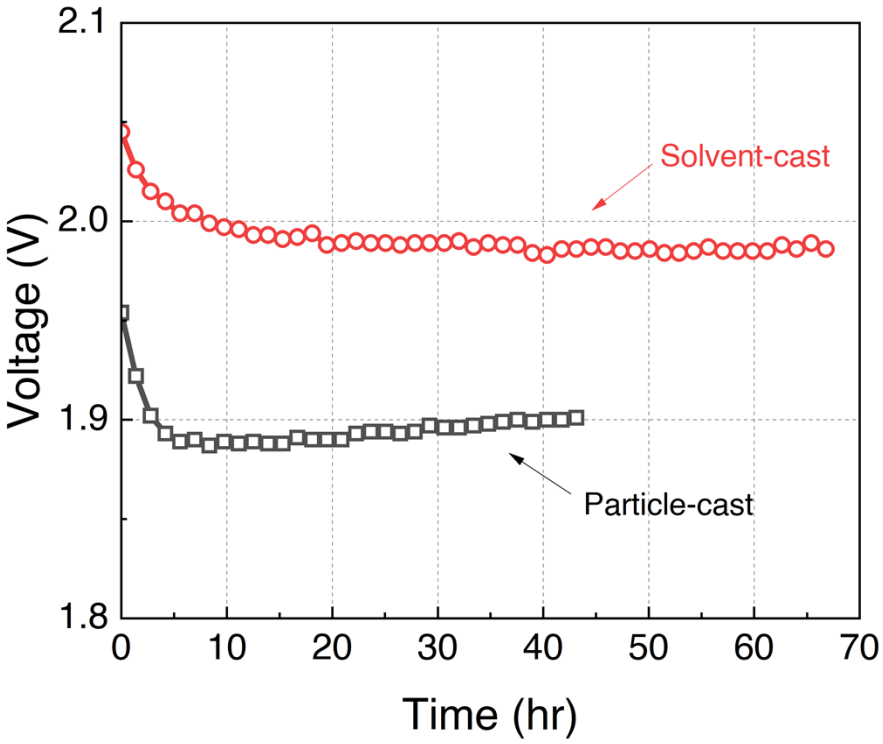

Figure 2. Voltage vs. time curve at 0.75 A/cm^2 for particle-cast and solvent-cast cathode with 30:45:25 ionomer. GT75-5 AEM (40 μm thick), 0.7 mg/cm^2 Pt_3Ni catalyst, and 0.65 mg/cm^2 NiFeOx anode catalyst on stainless steel PTL were used.

In Figure 2, the cathode catalyst, ionomer, and adhesive loadings in both experiments were the same (0.7 mg/cm^2 catalyst, 0.06 mg/cm^2 ionomer, and 0.18 mg/cm^2 adhesive). The 30:45:25 ionomer was used for the solvent-cast method. The IEC of the pre-aminated ionomer in the particle-cast cathode was 1.62 meq/g$^-$

, and the IEC of the soluble 30:45:25 ionomer was 2.28 meq/g after amination. Although the initial voltage for the particle-cast cathode in Figure 2 was lower than that for the solvent-cast electrode, the voltage for the particle-cast cathode increased steadily due to the observable detachment of catalyst from the PTL during the test. On the other hand, a more stable voltage profile was observed for the solvent-cast cathode.

In order to investigate the mechanism for the improved stability, the tape-test was used to show the enhanced adhesion with the solvent-cast method. Adhesive tape was firmly pressed onto each electrode and removed by pulling the tape off the surface at a 90^{o} angle to the plane of the electrode. With the particle-cast cathode, some parts of the active catalyst/ionomer layer were easily detached from the PTL and stuck to the tape. With the solvent-cast cathode, however, only a few isolated particles were stuck to the tape and most of the active materials remained on the PTL. These results demonstrate that the adhesion of active materials could be dramatically improved by use of a functionalized ionomer and epoxy additive in a soluble and homogeneous form in the electrode formulation, thereby mitigating the detachment and isolation problems of cathode catalyst and ionomer.

Figure 3 shows images of plane-view (Figure 3a and b) and cross-section view (Figure 3c and d) for the particle-cast (Figure 3a and c) and solvent-cast (Figure 3b and d) cathodes. The catalyst appears as bright particles in the cross-sections. Compared to the particle-cast method, the solvent-cast method deposits the catalyst to a greater depth within the electrode PTL. This is because there are fewer solids in the solvent-cast ink due to the soluble ionomer and adhesive. The particle-cast catalyst accumulates as a denser layer on the PTL, which could block the gas evolution pathway (Figure 3a and c) if it were too thick. The solvent-cast catalyst formed a more porous morphology, as shown in Figure 3b and d. This thick solvent-cast microstructure is beneficial for higher surface area electrodes improving the mass transfer within the electrode.

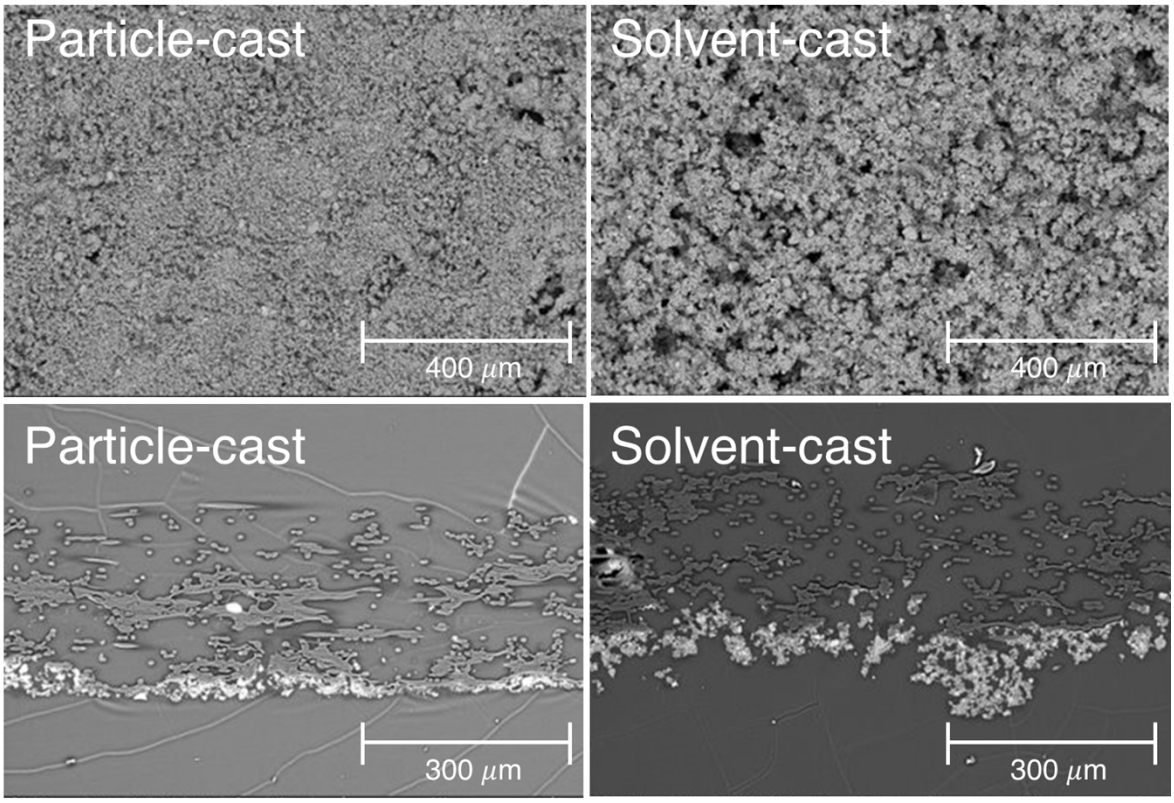

Figure 3. Plane-view (top images) and cross-sectional view (bottom images) of the particle-cast (left images) and solvent-cast cathodes (right images) used in the Figure 2.

It is noted that the ionomer IEC and catalyst loadings in this test (Figures 2 and 3) were previously optimized for the particle-cast electrode. [3] The introduction of the non-ionic epoxy adhesive to the electrode and dispersion of the solvated ionomer in the solvent-cast electrode makes its microstructure and ionic pathways significantly different from the particle-cast electrode. Thus, the composition of the solvent-cast ink was optimized for the solvent-cast method. The next phase of this study is to optimize the cathode solvent-cast formulation and explore the trade-offs between applied voltage and cell durability.

First, effect of mole fraction of the poly(norbornene) terpolymer ionomers within the electrode on the steady-state voltage response was investigated. Figure 4 shows a comparison of three solvent-cast cathodes using 50:35:15 (IEC = 1.89 meq/g), 40:40:20 (2.09 meq/g), and

30:45:25 (IEC = 2.28 meq/g) with the same mass loadings of the ionomer, adhesive, and cathode catalyst. GT72-10 AEM and 0.7 mg/cm^2 NiFeOx anode catalyst on nickel fiber PTL were used. By changing the ratio of the monomers within the terpolymer, the hydrophobicity and IEC was tuned. The three ionomers (40:40:20, 50:35:15, and 30-45-25) were compared, with all other materials and processes being the same. The 50:35:15 ionomer had the lowest IEC and was the most hydrophobicity of the three and had the highest initial voltage, as shown in Figure 4. The 40:40:20 ionomer had a higher IEC than the 50:35:15 ionomer, and the applied voltage trended toward that of 40:40:20 after a short period of time. The most effective ionomer was the one with the highest IEC, 30:45:25, showing the lowest steady-state voltage among the three. The mole ratio of the carboxylic acid norbornene within the polymer (15 to 25 mol%) did not appear to be a major differentiator. These results show that higher IEC and hydrophilicity are beneficial for the solvent-cast hydrogen cathode.

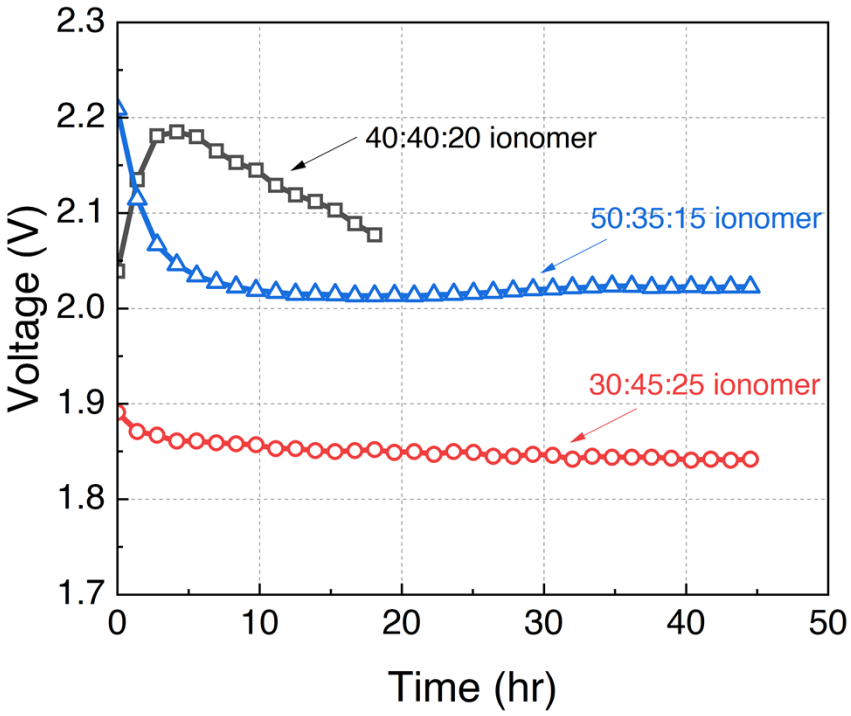

Figure 4. Voltage vs. time curve at 0.75 A/cm^2 for 50:35:15, 40:40:20, and 30:45:35 cathode ionomers. GT72-10 AEM, 1.1 mg/cm^2 Pt_3Ni catalyst, and 0.7 mg/cm^2 NiFeOx anode catalyst on Ni fiber (Dioxide Materials) were used.

It was found that increasing the IEC of ionomer even higher to 2.9 meq/g (20:60:20 ionomer) further improved the steady-state voltage at 0.75 A/cm^2, as shown in Figure 5a. The solvent-cast cathode contained Pt_3Ni catalyst (0.7 mg/cm^2), epoxy adhesive (0.06 mg/cm^2), and ionomer loading (0.18 mg/cm^2) on carbon paper PTL. The NiFeOx anode contained 0.7 mg/cm^2 catalyst, 0.11 mg/cm^2 adhesive, and 0.16 mg/cm^2 on stainless steel PTL). The membrane was 40 μm thick GT75-5 AEM. Figure 5b shows the beginning of life (EOL) and end of life (EOL) polarization curves for the celling using the 30:45:25 and 20:60:20 cathode ionomers from Fig. 5a. The higher IEC ionomer, 20:60:20, had a lower applied voltage in the low-current activation overpotential region and lower voltage in the high-current ohmic overpotential region due to the ionomer's higher water activity and lower ionic resistance compared to the 30:45:25 ionomer. The 20:60:20 ionomer could better bridge the ionic pathway between the bulk electrolyte and the cathode catalyst. It is also noted that the cells in Fig. 5 showed a similar break-in time.

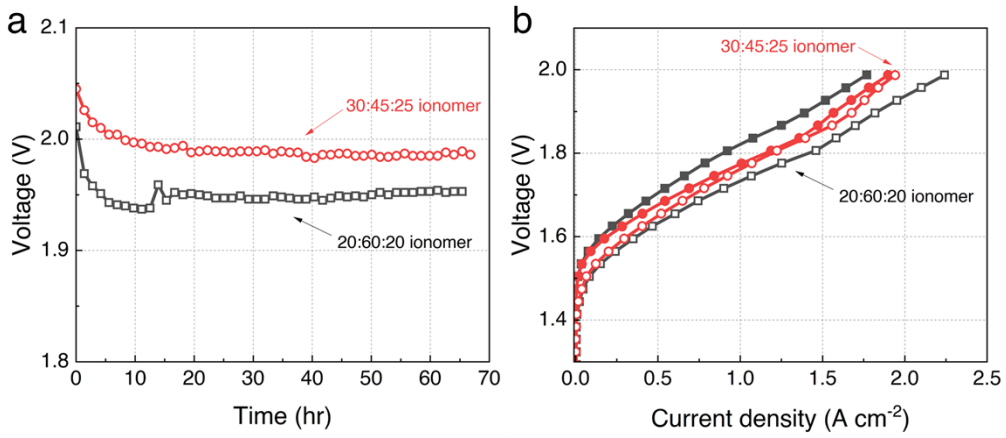

Figure 5. Comparison of 30:45:25 and 20:60:20 cathode ionomers. (a) Voltage vs. time curve at 0.75 A/cm^2. (b) Polarization curve (solid: BOL and open: EOL) at 5 mV/s scan rate. GT75-5 AEM, 0.7 mg/cm^2 Pt_3Ni cathode catalyst, and 0.7 mg/cm^2 NiFeOx anode catalyst on stainless steel PTL were used.

The effect of cathode catalyst loading on the steady-state voltage response was investigated using the 20:60:20 cathode ionomer with adhesive. Figure 6 shows the steady-state voltage at 1 A/cm^2 using four cathode catalyst loadings. The results show that a low catalyst loading, 0.4 mg/cm^2, resulted in a higher and noisy steady-state voltage. The noise was likely due to formation and discharge of hydrogen gas bubbles from the fewer catalyst sites in this electrode. By increasing the catalyst loading, the voltage fluctuation was lowered, as shown by the higher catalyst loading electrodes. In addition to smaller fluctuations in the voltage, the higher catalyst loading showed a lower applied voltage. It was also found that excess catalyst loading (>1.4 mg/cm^2), likely impeded transport through the electrolyte resulting in higher applied voltage. This is supported by the SEM cross-sections shown in Figure 7 where the catalyst particles (bright colored particles in Fig. 7) seem to close off channels through the PTL. Thus, moderate catalyst loadings (0.7 ~ 1.2 mg/cm^2) are favorable in terms of applied voltage response with the lowest steady-state voltage at 1.94 V with 1.2 mg/cm^2 catalyst loading.

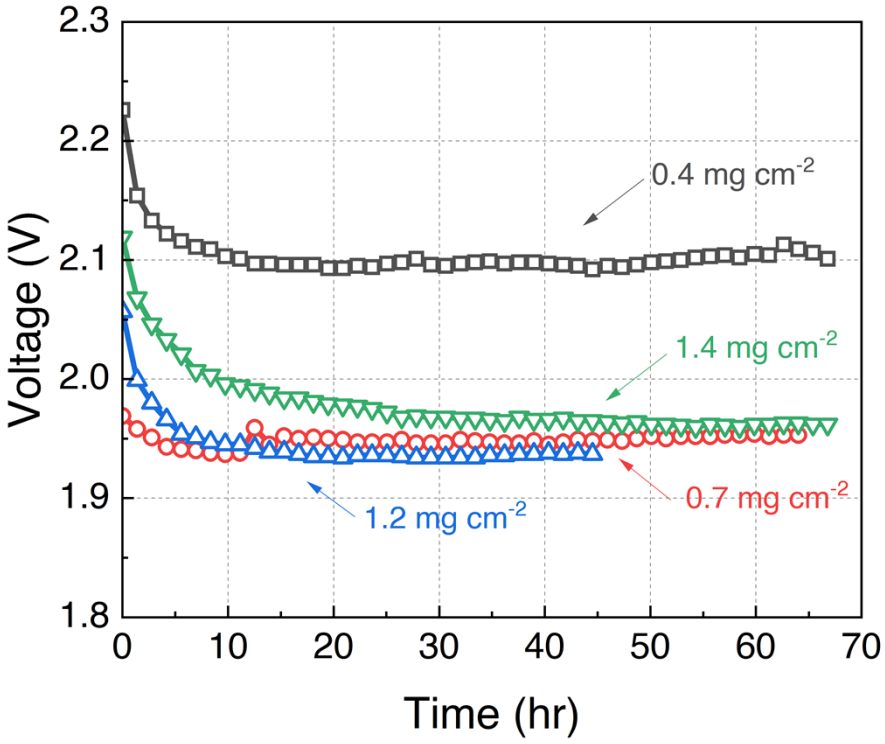

Figure 6. Voltage vs. time curve at 1 A/cm^2 for various Pt_3Ni cathode catalyst loadings. 20:60:20 cathode ionomer, GT75-5 AEM, 0.7 mg/cm^2 NiFeOx anode catalyst on stainless steel PTL were used.

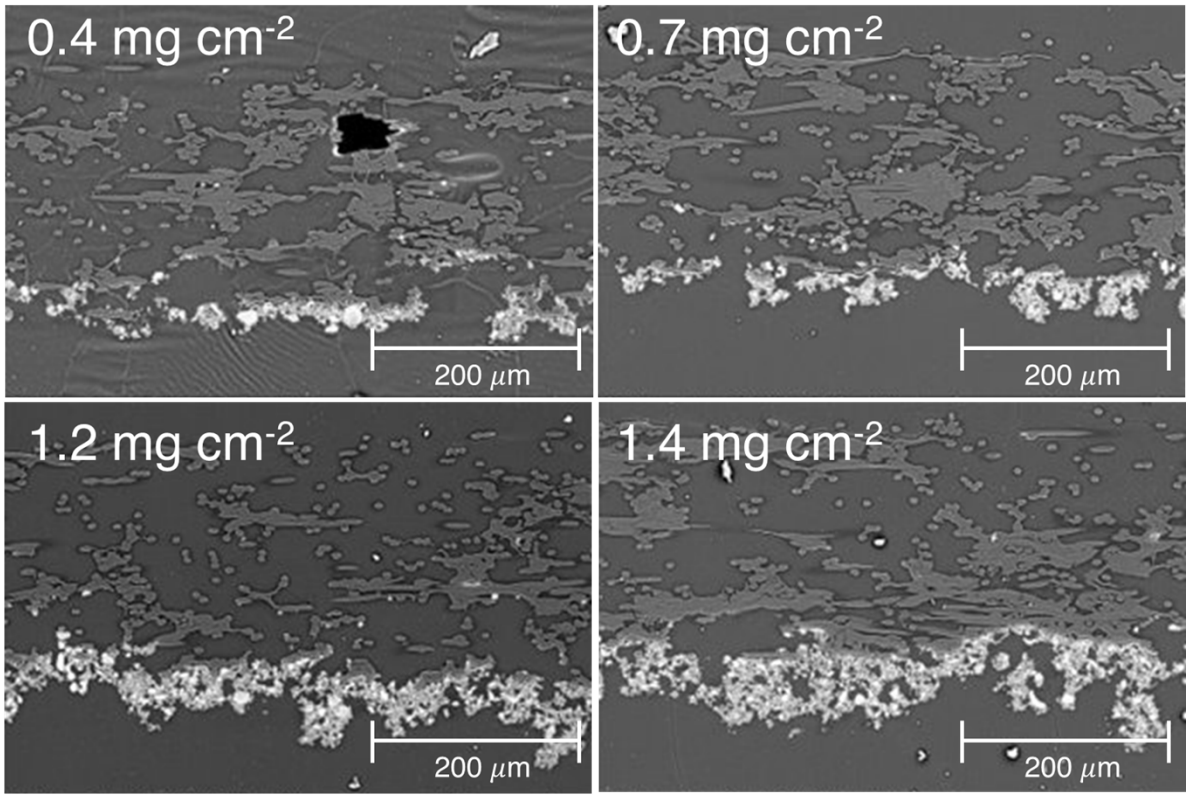

Figure 7. SEM cross-sections for the cathodes with different catalyst loadings of 0.4 mg/cm^2, 0.7 mg/cm^2, 1.2 mg/cm^2, and 1.4 mg/cm^2, used in Figure 6.

The effect of adhesive loading in the cathode on cell performance was studied by using the optimized ionomer (20:60:20) and catalyst loading (1.2 mg/cm^2). Three ionomer loading levels (0.3, 0.6, and 0.9 mg/cm^2) with constant adhesive loading (0.1 mg/cm^2), and two adhesive loadings (0.1 and 0.2 mg/cm^2) with constant ionomer loading (0.6 mg/cm^2) were compared, as shown in Figure 8. A moderate ionomer loading, 0.6 mg/cm^2 with 0.1 mg/cm^2 adhesive loading gave the lowest steady-state voltage (1.88 V). Ionomer loading of 0.3 mg/cm^2 gave the higher steady-state voltage (1.94 V), which is likely due to insufficient ionic transport within the electrode. Higher ionomer loading (e.g., 0.9 mg/cm^2) or higher adhesive loading (e.g., 0.2 mg/cm^2) led to higher applied voltage which is most likely due to catalyst coverage and deactivation. Increasing the loading of adhesive from 0.1 to 0.2 mg/cm^2 with the same ionomer loading (0.6 mg/cm^2) resulted in poorer performance because the adhesive forms covalent bonds with ionomer, catalyst, and PTL.

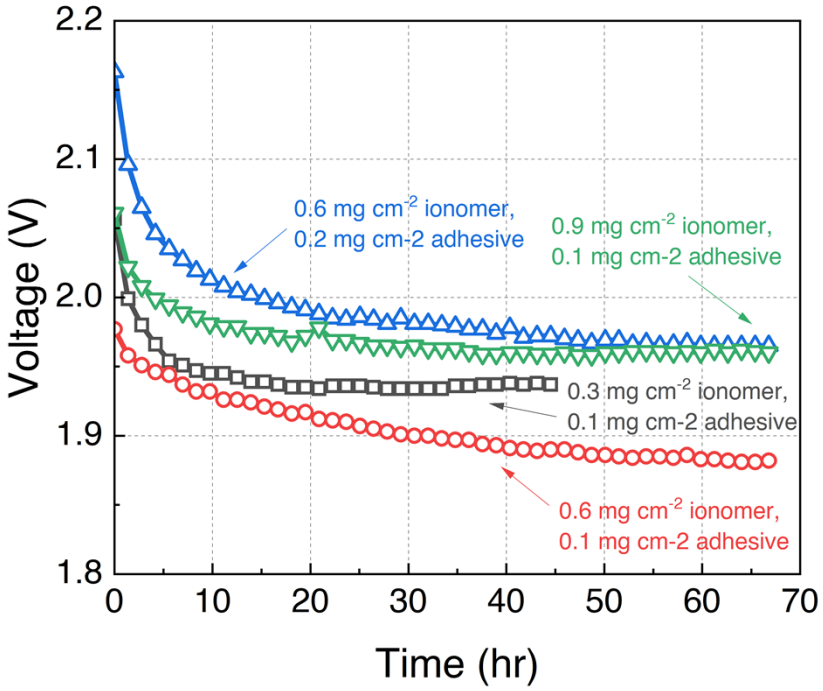

Figure 8. Voltage vs. time curve at 0.75 A/cm^2 for various ionomer and adhesive loadings. GT75-5 AEM, 20:60:20 cathode ionomer, 1.2 mg/cm^2 Pt_3Ni cathode catalyst, and 0.7 mg/cm^2 NiFeOx anode catalyst on stainless steel PTL were used.

.

The results from the loading studies were used to make an optimized solvent-cast cathode (1.2 mg/cm^2 catalyst, 0.6 mg/cm^2 ionomer, and 0.1 mg/cm^2 adhesive) as shown in Figure 9. The cell was run at 1 A/cm^2 for the first 45 hr and the steady-state voltage was 1.82 V. This compares favorably to the particle-cast cathode in Figure 2 whose volage was ca. 1.9 V and degraded at a rate of 402 μV/hr. The cell with optimized solvent-cast cathode was then operated at 1.5 A/cm^2 with a steady-state voltage of 1.91 V. The electrolyte was refreshed at the 73 hr mark to see the effect of higher current density and cycling off/on. The initial voltage after electrolyte refreshment was 1.89 V but recovered to the original of 1.91 V, within 20 hr. This transient effect is likely due to removal of bubbles on the anode or cathode during the rest period. Minor fluctuations in voltage were observed which are likely due to gas bubble accumulation at high

current density. It is important to note that the applied voltage did not degrade from the original 1.91 V during the 90 hr test at 1.5 A/cm^2.

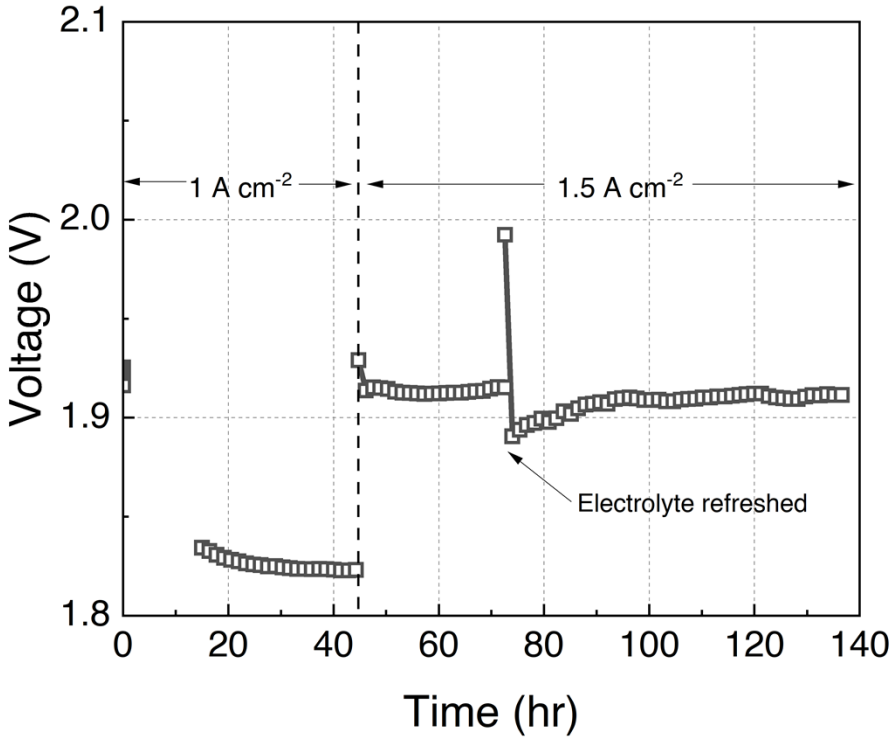

Figure 9. Voltage vs. time curve at 1 A/cm^2 for first 45 hrs and at 1.5 A/cm^2 for next 90 hr. GT75-5 AEM, 1.2 mg/cm^2 Pt_3Ni cathode catalyst, 0.6 mg/cm^2 20:60:20 cathode ionomer, 0.1 mg/cm^2 adhesive, and NiFeOx anode optimized on Ni fiber PTL (Technetics Group) were used. The 0.1 M NaOH electrolyte was refreshed at the 73 hr mark.

Conclusions

A self-adhesive cathode ionomer was developed for IEC and hydrophobicity for use in an AEM alkaline electrolyzer. The cathode ionomer, catalyst, and adhesive loadings were optimized to improve the steady-state electrolysis performance. Particle-cast cathodes made from insoluble ionomers resulted in poor catalyst adhesion and durability. Self-adhesive, soluble terpolymer ionomers were used and showed little or no degradation in >100 hr tests with cell voltage of 1.82 V at 1 A/cm^2 and 1.91 V at 1.5 A/cm^2. The addition of a non-ionic adhesive to the catalyst-ionomer ink resulted in excellent cathode durability due to the covalently bonded ionomers with

the catalyst and PTL. This study highlights the design of the self-adhesive ionomer and optimization of electrode loadings.

Acknowledgements

The authors gratefully acknowledge the financial support of the U.S. Department of Energy, Office of Energy Efficiency & Renewable Energy H2@Scale program (Award Number: DE-EE0008833).

References

1. Zeng, K.; Zhang, D., Recent progress in alkaline water electrolysis for hydrogen production and applications. *Progress in Energy and Combustion Science* **2010,** *36* (3), 307-326.

2. Li, X.; Walsh, F. C.; Pletcher, D., Nickel based electrocatalysts for oxygen evolution in high current density, alkaline water electrolysers. *Physical Chemistry Chemical Physics* **2011,** *13* (3), 1162-1167.

3. Huang, G., Mandal, M., Hassan, N., Groenhout, K., Dobbs, A., Mustain, W., and Kohl, P. A., "Ionomer Optimization for Water Uptake and Swelling in Anion Exchange Membrane Electrolyzer: Hydrogen Evolution Electrode", Journal of the Electrochemical Society, 168, 024503 (2021).

4. Pérez-Alonso, F. J.; Adán, C.; Rojas, S.; Peña, M. A.; Fierro, J. L. G., Ni/Fe electrodes prepared by electrodeposition method over different substrates for oxygen evolution reaction in alkaline medium. *International Journal of Hydrogen Energy* **2014,** *39* (10), 5204-5212.

5. Shalom, M.; Ressnig, D.; Yang, X.; Clavel, G.; Fellinger, T. P.; Antonietti, M., Nickel nitride as an efficient electrocatalyst for water splitting. *Journal of Materials Chemistry A* **2015,** *3* (15), 8171-8177.

6. Herraiz-Cardona, I.; González-Buch, C.; Valero-Vidal, C.; Ortega, E.; Pérez-Herranz, V., Co-modification of Ni-based type Raney electrodeposits for hydrogen evolution reaction in alkaline media. *Journal of Power Sources* **2013,** *240*, 698-704.

7. Phillips, R.; Edwards, A.; Rome, B.; Jones, D. R.; Dunnill, C. W., Minimising the ohmic resistance of an alkaline electrolysis cell through effective cell design. *International Journal of Hydrogen Energy* **2017,** *42* (38), 23986-23994.

8. Pletcher, D.; Li, X.; Wang, S., A comparison of cathodes for zero gap alkaline water electrolysers for hydrogen production. *International Journal of Hydrogen Energy* **2012,** *37* (9), 7429-7435.

9. Kraglund, M. R.; Aili, D.; Jankova, K.; Christensen, E.; Li, Q.; Jensen, J. O., Zero-Gap Alkaline Water Electrolysis Using Ion-Solvating Polymer Electrolyte Membranes at Reduced KOH Concentrations. *Journal of The Electrochemical Society* **2016,** *163* (11), F3125-F3131.

10. Carmo, M.; Fritz, D. L.; Mergel, J.; Stolten, D., A comprehensive review on PEM water electrolysis. *International Journal of Hydrogen Energy* **2013,** *38* (12), 4901-4934.

11. Ursua, A.; Gandia, L. M.; Sanchis, P., Hydrogen Production From Water Electrolysis: Current Status and Future Trends. *Proceedings of the IEEE* **2012,** *100* (2), 410-426.

12. Millet, P.; Mbemba, N.; Grigoriev, S. A.; Fateev, V. N.; Aukauloo, A.; Etiévant, C., Electrochemical performances of PEM water electrolysis cells and perspectives. *International Journal of Hydrogen Energy* **2011,** *36* (6), 4134-4142.

13. Mandal, M., Huang, G., and Kohl, P. A., "Highly Conducting Anion-Exchange Membranes Based on Cross-linked Poly(norbornene): Vinyl Addition Polymerization", ACS Journal of Applied Energy and Materials, 2, 2447-2457 (2019).

14. Mandal, M., Huang, G., and Kohl, P. A., "Anionic Multiblock Copolymers Based on Vinyl Addition Polymerization of Norbornenes: Applications in Anion-Exchange Membrane Fuel Cells", Journal of Membrane Science, 5670-5671, 394-402 (2019).

15. Babic, U.; Suermann, M.; Büchi, F. N.; Gubler, L.; Schmidt, T. J., Critical Review—Identifying Critical Gaps for Polymer Electrolyte Water Electrolysis Development. *Journal of The Electrochemical Society* **2017,** *164* (4), F387-F399.

16. Li, H.; Inada, A.; Fujigaya, T.; Nakajima, H.; Sasaki, K.; Ito, K., Effects of operating conditions on performance of high-temperature polymer electrolyte water electrolyzer. *Journal of Power Sources* **2016,** *318*, 192-199.

17. Li, D.; Park, E. J.; Zhu, W.; Shi, Q.; Zhou, Y.; Tian, H.; Lin, Y.; Serov, A.; Zulevi, B.; Baca, E. D.; Fujimoto, C.; Chung, H. T.; Kim, Y. S., Highly quaternized polystyrene ionomers for high performance anion exchange membrane water electrolysers. *Nature Energy* **2020**.

18. Ren, R., Zhang, S., Miller, H., Vizza, F., Varcoe, J. R., and He, Q., Facile Preparation of and Ether-Free Anion Exchange Membrane with Pendant Cyclic Quaternary Ammonium Groups, *ACS Applied Energy Materials,* **2019**, 2, 4576-4581.

19. Buttler, A.; Spliethoff, H., Current status of water electrolysis for energy storage, grid balancing and sector coupling via power-to-gas and power-to-liquids: A review. *Renewable and Sustainable Energy Reviews* **2018,** *82*, 2440-2454.

20. Pavel, C. C.; Cecconi, F.; Emiliani, C.; Santiccioli, S.; Scaffidi, A.; Catanorchi, S.; Comotti, M., Highly Efficient Platinum Group Metal Free Based Membrane-Electrode Assembly for Anion Exchange Membrane Water Electrolysis. *Angewandte Chemie International Edition* **2014,** *53* (5), 1378-1381.

21. Bessarabov, D.; Millet, P.; Pollet, B. G., *PEM Water Electrolysis*. Elsevier Science: 2018.

22. Vincent, I.; Kruger, A.; Bessarabov, D., Hydrogen Production by water Electrolysis with an Ultrathin Anion-exchange membrane (AEM). *International Journal of Electrochemical Science* **2018,** *13*, 11347-11358.

23. Noor, U., Mandal, M., Huang, G., Firouzja, H., Kohl, P. A., and Mustain, W., "Achieving High-Performance and 2000 h Stability in Anion Exchange Membrane Fuel Cells by Manipulating Ionomer Properties and Electrode Optimization", Advanced Energy Materials, 10, 10.1002/aenm.202001986 (2020).

24. Huang, G.; Mandal, M.; Hassan, N. U.; Groenhout, K.; Dobbs, A.; Mustain, W. E.; Kohl, P. A., Ionomer Optimization for Water Uptake and Swelling in Anion Exchange Membrane Electrolyzer: Oxygen Evolution Electrode. *Journal of the Electrochemical Society* **2020,** *167* (16), 164514.

25. Ahlfield, J.; Huang, G.; Liu, L.; Kaburagi, Y.; Kim, Y.; Kohl, P. A., Anion Conducting Ionomers for Fuel Cells and Electrolyzers. *Journal of The Electrochemical Society* **2017,** *164* (14), F1648-F1653.